

# “Spin-Hall Effect”: From the Ballistic to the Diffusive Regime

*Roksana Golizadeh-Mojarad<sup>1</sup> and Supriyo Datta<sup>2</sup>*  
*School of Electrical and Computer Engineering,*  
*and the NSF Network for Computational Nanotechnology*  
*Purdue University, West Lafayette, IN-47906, USA.*

(Date: March 9, 2007)

The “spin-Hall effect” has recently attracted a lot of attention and a central question is whether the effect is due to the *intrinsic* spin-orbit interaction or due to spin-asymmetric scattering by *extrinsic* impurities. The objective of this paper is to shed light on this question using a new approach based on the non-equilibrium Green function (NEGF) formalism, which allows us to go continuously from the ballistic to the diffusive limit and we present approximate analytical expressions that describe our results fairly well. Our model suggests that a spin accumulation proportional to the current should be observed even in clean ballistic sample. We further show good quantitative agreement with recent experimental observations in GaAs suggesting that these can be understood in terms of an intrinsic effect driven by the Rashba interaction, although experiments on ZnSe likely have a different origin.

The “spin-Hall effect” [1] has attracted a lot of attention, especially following recent experimental observations of the effect, both optically [2, 3, 4] and electronically [5]. One central issue regarding the underlying mechanism is whether the effect is due to the *intrinsic* spin-orbit interaction or due to spin-asymmetric scattering by *extrinsic* impurities and the answer is not yet clear [6]. Theoretically, the question has been addressed largely using the Kubo formalism [7, 8], the drift-diffusion formulation [9] and very recently the scattering theory of transport [10]. The objective of this paper is to shed light on this question using a very different approach based on the non-equilibrium Green function (NEGF) method [11, 12]. This NEGF-based quantitative model allows us to study the evolution of the effect continuously from the ballistic to the diffusive limit. We use quotes around “spin-Hall effect” since this term is usually associated with the existence of a non-zero bulk spin conductivity tensor [7, 8], which is calculated from microscopic theory [1] and can then be used in a macroscopic transport theory. We do not calculate this tensor and as such do not offer any insights regarding it. Instead, we use our NEGF-based approach to connect directly from a microscopic Hamiltonian to the macroscopic effects that are actually observed in experiments, namely an accumulation of spin-up and spin-down electrons at the opposite edges of a finite-sized sample. We call this a “spin-Hall effect” simply by its analogy with the normal Hall effect, which involves the accumulation and depletion of charges at opposite edges (see Fig. 1). In either case, the accumulation (spin or charge) vanishes for zero current and is proportional to the current at least for low bias.

**Model:** We consider a two-dimensional conductor described by a single-band effective mass ( $m^*$ ) Hamiltonian

$$H_0 \equiv (p_x^2 / 2m^*) + (p_y^2 / 2m^*) + U(y), \quad (1)$$

with a confinement potential  $U(y)$  along with an additional spin-orbit interaction assumed to have the Rashba form

$$H \equiv H_0 I + \frac{\alpha}{\hbar} (\sigma_x p_y - \sigma_y p_x). \quad (2)$$

We have also investigated the effect of Dresselhaus interactions and edge potentials [13], and find interesting differences like sign reversal, but in this paper we will focus on the Rashba interaction. We study the spin accumulation in this conductor in different transport regimes, from ballistic to diffusive, using the NEGF approach, which has been described elsewhere in detail [11, 12]. Here we simply note that for diffusive transport, incoherent scattering is introduced through the uncorrelated point scatterer model [11] (Note:  $\Sigma^{in} \equiv -i\Sigma^<$ ,  $G^n \equiv -iG^<$ ,  $G \equiv G^R$ ,  $\Sigma \equiv \Sigma^R$ )

$$\Sigma_s^{in}(r, r'; E) = D_0 [G^n(r, r; E)] \delta(r - r'), \quad (3a)$$

$$\Sigma_s(r, r'; E) = D_0 [G(r, r; E)] \delta(r - r'), \quad (3b)$$

where the parameter  $D_0$  is adjusted to obtain different strengths of scattering leading to different mean free paths. Note that this particular model provides both momentum and spin relaxation, so that the mean free path  $L_m$  is essentially the same as the spin coherence length  $L_S$ . A different choice for the D-matrix relating  $\Sigma$  to  $G$  [11] could allow independent control of spin and momentum relaxation, but we leave that for future work.

---

<sup>1</sup> rgolizad@purdue.edu

<sup>2</sup> datta@purdue.edu

**“Spin-Hall” versus normal Hall effect:** To clarify our model and what we mean by “spin-Hall effect”, we start by comparing it with the normal Hall effect for a ballistic ( $D_0 = 0$ ) rectangular conductor modeled using identical parameters [Fig. 1(a,b)] chosen to correspond to the GaAs epilayer used in [2]:  $m^* = 0.07 m_e$  ( $m_e$ : free electron mass),  $\alpha = 1.8 \text{ meV} - nm$  (as measured in [14]),  $k_f \approx 10^8 \text{ m}^{-1}$  corresponding to an electron density of  $n = k_f^3 / 3\pi^2 \approx 3 \times 10^{16} \text{ cm}^{-3}$ ,  $E_f = 5 \text{ meV}$ . Fig. 1(a) shows the net z-directed spin density per unit applied bias (with no magnetic field present). Fig. 1(b) shows the *change* in the electron density per unit applied bias relative to the equilibrium (zero bias) electron density with a fixed magnetic field  $B$  ( $= 0.05T$ ), in the -z-direction which was included in Eq. (1) through a vector potential following the usual prescription [15]. The oscillations in either case correspond to the Fermi wavenumber and are smoothed out on averaging over a range of energies  $\sim \pm 2.5 \text{ meV}$  ( $\sim k_B T$ ,  $T = 30\text{K}$ ) as shown. We find that the linear accumulation across the sample is described approximately by  $(-W/2 < y < +W/2)$

$$\tilde{n}_z(y, E) \approx (k_\alpha / \pi)^2 (M(E)/E) (-2y/W), \quad (4a)$$

for spin (z-directed) accumulation in the “spin-Hall effect” and by

$$\tilde{n}(y, E) \approx (eB / \pi\hbar) (M(E)/E) (2y/W), \quad (4b)$$

for electron accumulation in the normal Hall effect. Here  $k_\alpha \equiv m^* \alpha / \hbar^2$  is the spin precession wave vector and  $M(E)$  is the number of transverse modes or subbands (including spin) which can be estimated from the expression  $M = 2kW/\pi$ ,  $k$  being the electron wavenumber ( $= \sqrt{2m^* E / \hbar}$ ). Eqs. (4a,b) describe our results for a ballistic conductor fairly well and can be justified from a Landauer approach as described below. We can relate the electron accumulation to a Hall voltage  $V_H$  through the 2-D density of states to write  $V_H = V_A [\tilde{n}]_{\max} / (m^* / \pi\hbar^2)$ . Noting that the current  $I$  is related to the applied bias  $V_A$  through  $I = (e/h) M(E) V_A$ . It is straightforward to show that the Hall resistance deduced from Eq. (4b) agrees with the standard result  $(B/e n_s)$ . When we use our NEGF-based approach to introduce incoherent scattering processes, we find that the spin (electron) accumulation is localized within a few mean free paths  $L_m$  near the edges (note that in our model  $L_m$  is essentially the same as the spin coherence length  $L_S$ ). The magnitude is still well described by Eqs. (4a,b) provided we replace the applied voltage with an effective voltage equal to the voltage drop across a mean free path, as explained later in this paper.

The maximum spin accumulation at the edge can be written from Eq. (4a) as

$$[\tilde{n}_z]_{\max} \approx (m^* / \pi\hbar^2) (k_\alpha / k_f) (k_\alpha W / \pi). \quad (5a)$$

For values of  $k_\alpha W > 1$ , however, the spin accumulation does not increase quadratically with  $k_\alpha$  as predicted by Eq.(5a) and is better described by a linear increase ( $k_\alpha / k_f < 1$ )

$$[\tilde{n}_z]_{\max} \approx (m^* / \pi\hbar^2) (k_\alpha / k_f) (1/2\pi). \quad (5b)$$

More importantly, the spin accumulation is localized near the edges reminiscent of edge states in the quantum Hall regime. Indeed the similarity between Eqs. (4a,b) suggests that for the “spin-Hall effect”, the quantity  $1/k_\alpha$  plays a role analogous to the magnetic length  $\sqrt{\hbar/eB}$  in the normal Hall effect and it seems natural to expect a qualitative change when the quantity  $k_\alpha W \gg 1$ . For the examples presented in this paper, however,  $k_\alpha W \leq 1$ .

**Landauer approach:** Although our numerical results are obtained from an NEGF-based model, it is instructive to note that Eqs. (4a,b) for a ballistic conductor can be justified from a Landauer viewpoint. We can show that for current flow along x in a clean intrinsic two-dimensional conductor, the accumulated spin density  $n_z(y)$  along the transverse direction y can be written as

$$n_z(y) = \int dE \tilde{n}_z(y, E) [f_1(E) - f_2(E)]. \quad (6)$$

Note the similarity of Eq. (6) with the standard expression for the current in a ballistic conductor in the Landauer framework [15]

$$I = (e/h) \int dE M(E) [f_1(E) - f_2(E)]. \quad (7)$$

Eq. (7) is obtained by arguing that for every eigenstate  $\exp(+ik_x x)$  there is a degenerate eigenstate  $\exp(-ik_x x)$  carrying current in the opposite direction. At equilibrium both eigenstates are equally occupied giving zero net current, but under bias they are occupied from the two contacts with different Fermi functions  $f_1$  and  $f_2$  giving rise to a net current given by Eq. (7). We can similarly argue that for every eigenstate of H [Eq. (2)] ( $L$ : normalization length along x-direction)

$$\begin{Bmatrix} p(y) \\ q(y) \end{Bmatrix} (1/\sqrt{L}) \exp(+ik_x x), \quad (8a)$$

with a net z-directed spin of  $|p(y)|^2 - |q(y)|^2$ , there is a degenerate eigenstate

$$\begin{Bmatrix} q(y) \\ p(y) \end{Bmatrix} (1/\sqrt{L}) \exp(-ik_x x), \quad (8b)$$

with the opposite spin distribution  $|q(y)|^2 - |p(y)|^2$ . At equilibrium, both eigenstates are occupied and there is no spin accumulation. But under bias, these states are unequally occupied according to different Fermi functions  $f_1$  and  $f_2$  giving a net spin accumulation described by Eq.(6), with the function

$$\tilde{n}_z(y, E) dE = \sum_{E \leq \varepsilon(n, k_x) \leq E + dE} (1/L) \left[ |p(y)|^2 - |q(y)|^2 \right]_{n, k_x}, \quad (9)$$

obtained by summing the spin accumulation due to each eigenstate having an energy  $\varepsilon(n, k_x)$  lying between  $E$  and  $E+dE$ . The sign of the spin accumulation alternates between subbands ‘ $n$ ’ but when summed over a large number of modes the function  $\tilde{n}_z(y, E)$  is approximated well by the simple expression given in Eq. (4a). Eq. (4b) for the normal Hall effect can also be obtained from the same approach, indeed more simply since the wavefunctions for all eigenstates with  $k_x > 0$  are shifted to one edge while those for eigenstates with  $k_x < 0$  are shifted to the other edge [ Ref. 15, p. 37]. There is thus no alternation in the signs of the terms appearing in the normal Hall version of Eq. (9), making Eq.(4b) relatively straightforward to obtain.

**Diffusive transport:** We can also use the ballistic result in Eq. (4a) to understand spin accumulation in the diffusive regime appropriate for all recent experimental results if we make two important replacements. **Firstly**, the width  $W$ , which enters Eq. (4a) through  $M \approx 2k_f W / \pi$  should be replaced by an effective width determined by the spin coherence length

$$W_{\text{eff}} = (WL_S / (W + L_S)) \sim L_S. \quad (10a)$$

**Secondly**, for a diffusive sample we should use an effective voltage obtained by scaling down the full voltage  $V_A$  applied across the length of the conductor  $L$  by the factor  $L_m / (L + L_m)$ ,  $L_m$  being the momentum relaxation length ( $F$ : electric field):

$$eV_{\text{eff}} = eV_A L_m / (L + L_m) = eF L L_m / (L + L_m) \quad (10b)$$

This can be justified by noting that in a diffusive sample the separation in the electrochemical potentials for  $+k$  and  $-k$  states is  $L_m / (L + L_m)$  times the applied voltage [Ref. 15, p. 75].

**Numerical results:** Fig. 2(a) shows one of the structures studied experimentally in Ref. 2. At positive values of  $x$ , the only edges are at the two ends, while for negative values of  $x$ , there is a notch in the middle with two additional edges. Fig. 2(c) shows the spin accumulation measured using Kerr rotation spectroscopy adapted from Ref. 2. The calculated spin density in Fig. 2(d) looks very similar in shape to the experimental results (including the “anticipatory” effect

ahead of the notch) and also agrees with the **sign** of the effect. Note that while the experimental structure has dimensions  $\sim 50 \mu\text{m}$ , the structure studied theoretically has dimensions  $\sim 150 \text{ nm}$ . However, in the theoretical model we have deliberately introduced a large amount of scattering such that the spin coherence length,  $L_s \sim 20 \text{ nm}$ , making the ratio  $L_s/W$  comparable to the experimental structure. The unusually short  $L_s$  also lowers the magnitude of the spin accumulation relative to Fig. 2(b), which shows the energy-averaged result for ballistic transport. The reduction agrees with Eq. (10a).

Note that the experimental results for the spin density were measured optically at the surface of a GaAs layer,  $2 \mu\text{m}$  thick, while our theoretical results are obtained for a two-dimensional conductor whose parameters ( $m^*$ ,  $k_f$  and  $\alpha$ ) are chosen to reflect those for the experimental structure, as mentioned earlier. We are using a Rashba coefficient  $\alpha = 1.8 \times 10^{-12} \text{ eV}\cdot\text{m}$  appropriate for confined GaAs layers, assuming that this is representative of the conditions at the surface of a bulk sample. This seems justifiable since the numerical simulations show that the effect of an edge extends a distance  $\sim L_s$  and the experimental layer thickness is only a fraction of  $L_s$ .

In order to compare the magnitude of spin accumulation, we note that  $F = 10 \text{ meV}/\mu\text{m}$ ,  $L_m = 0.7 \mu\text{m} \ll L$  (assuming a mobility of  $10^5 \text{ cm}^2/\text{V}\cdot\text{sec}$ ) so that  $eV_{\text{eff}} = 7 \text{ meV}$  from Eq.(10). Multiplying the calculated spin accumulation per unit bias from Fig. 2(d) by  $eV_{\text{eff}}$  we obtain a spin accumulation of  $\sim .14$  spins per  $\mu\text{m}^2$ . Scaling up by  $L_s$  [note that  $L_s \approx 9 \mu\text{m}$  (experimental),  $L_s \approx 20 \text{ nm}$  (numerical)] yields  $\sim 63$  spins per  $\mu\text{m}^2$  which is comparable or larger than the spin accumulation observed experimentally, suggesting that the experiments can be understood without invoking additional effects.

Two more interesting structures (see Fig. 3 and 4) studied in Ref. 2 show the diffusion of the accumulated spin away from the main current path into protruding sidearms and these are also in good agreement with our numerical model, especially when the spin coherence length is adjusted to have the same ratio  $L_s/W$  as the experimental structures [Figs. (3-4)].

**Summary and conclusions:** We have presented numerical results showing striking similarity to recent experimental observations of the “spin-Hall effect” in GaAs [2]. These are obtained from an NEGF-based model that allows us to go continuously from the ballistic to the diffusive limit. An approximate expression [Eq. (4)] is presented for the spin accumulation that describes the numerical results fairly well in the ballistic limit and simple relationships [Eqs. (10a,b)] are suggested for translating it to the diffusive limit. Our

model suggests a spin accumulation proportional to the current should be observed even in clean ballistic samples. We further show with considering the same parameter as mentioned in the experiment, our theoretical equation yields spin accumulation in the same order of magnitude as the spin accumulation observed experimentally. These suggest that the experimental observations in GaAs can be understood in terms of an intrinsic “spin-Hall effect” driven by the Rashba interaction, although those for ZnSe [16] likely have a different origin since the sign of the spin accumulation is reversed. Finally, we note that for a specified carrier density (and hence  $k_f$ ), Eq. (5b) predicts a spin accumulation  $\sim \alpha m^*{}^2$ , suggesting that a weak spin-orbit coupling could be compensated for by a large effective mass  $m^*$ , as in say Silicon ( $\alpha \approx 0.4 \text{ meV-nm}$ , [16]).

**Acknowledgements:** This work was supported by the MARCO focus center on Materials, Structure and Devices and the NSF Network for Computational Nanotechnology (NCN).

1. For recent review, see H. Engel, E. I. Rashba, B. I. Halperin, cond-mat/0603306, Sept 2006.
2. V. Sih, W. H. Lau, R. C. Myers, V. R. Horowitz, A. C. Gossard, and D. D. Awschalom, Phys. Rev. Lett. **97**, 096605 (2006).
3. J. Wunderlich, B. Kaestner, J. Sinova, T. Jungwirth, Phys. Rev. Lett. **94**, 047204 (2005).
4. Y. K. Kato, R. C. Myers, A. C. Gossard, and D. D. Awschalom, Science **306**, 1910 (2004).
5. S. O. Valenzuela and M. Tinkham, Nature **442**, 176 (2006).
6. V.M. Galitski, A.A. Burkov, and S. Das Sarma, Phys. Rev. B **74**, 115331 (2006).
7. J. Sinova, D. Culcer, Q. Niu, N. A. Sinitsyn and A. H. MacDonald, Phys. Rev. Lett. **92**, 126603 (2004).
8. S. Murakami, N. Nagaosa, and S. C. Zhang, Science **301**, 1348 (2003).
9. Wang-Kong Tse, J. Fabian, I. Zutic, and S. Das Sarma, Phys. Rev. B **72**, 241303 (2005).
10. Wei Ren, Zhenhua Qiao, Jian Wang, Qingfeng Sun and Hong Guo, Phys. Rev. Lett. **97**, 066603 (2006).
11. R. Golizadeh-Mojarad and S. Datta, Phys. Rev. B (Rapid Comm.) **75**, 081301 (2007).
12. S. Datta, Quantum Transport: Atom to Transistor (Cambridge University Press, Cambridge, 2005).
13. K. Suzuki and S. Kurihara, cond-mat/0611013, Nov 2006.
14. V. Sih, R. C. Myers, Y. Kato, W. H. Lau, A. C. Gossard, and D. D. Awschalom, Nature Phys. **1**, 31 (2005).
15. S. Datta, Electronic Transport in Mesoscopic Systems (Cambridge University Press, Cambridge, 1997).
16. N. P. Stern, S. Ghosh, G. Xiang, M. Zhu, N. Samarth, and D. D. Awschalom, Phys. Rev. Lett. **97**, 126603 (2006).
17. Chales Tahan and Robert Joynt, Phys. Rev. B **71**, 075315 (2005).

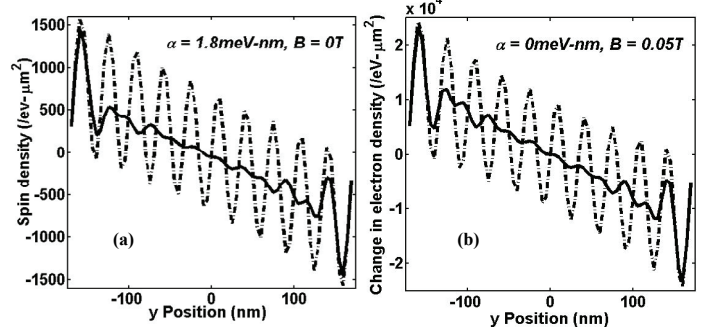


FIG. 1. Comparison of the “spin-Hall effect” (a) with the normal Hall effect (b) in a rectangular ballistic sample. Both calculations are based on the NEGF-based model described in Ref. [11,12]. Dashed line: single energy calculation; solid line: average over energy range of  $E_f \pm k_B T$  calculation ( $E_f = 5 \text{ meV}$ ,  $T = 30 \text{ K}$ ).

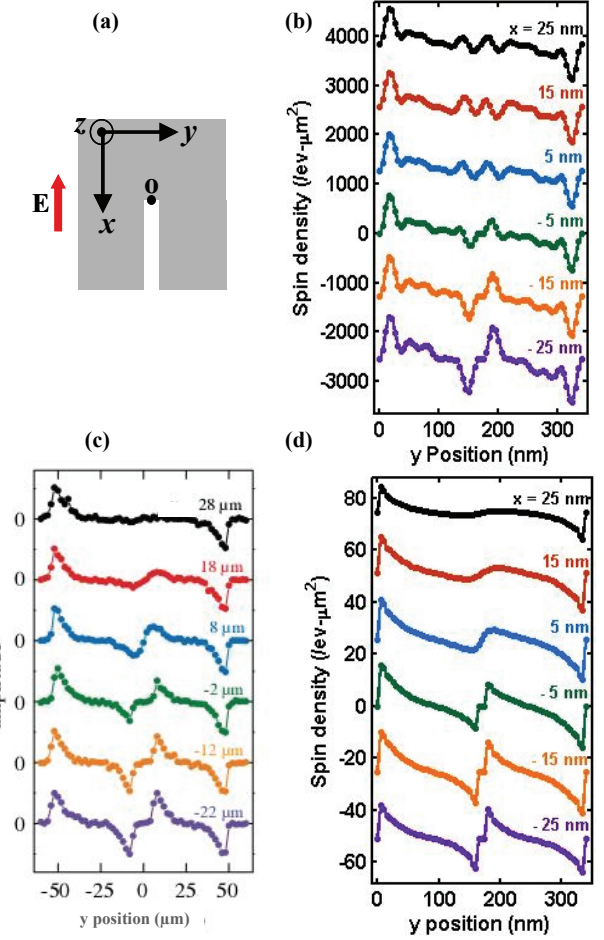


FIG. 2. (a) Schematic showing a channel that splits into two smaller channels.  $O$  indicates the origin. (b) NEGF-based calculated spin density in ballistic regime averaged over energy range of  $E_f \pm k_B T$  as a function of transverse position  $y$  for different longitudinal position  $x$  ( $E_f = 5 \text{ meV}$ ,  $T = 30 \text{ K}$ ). (c) Measured Kerr rotation amplitude as a function of transverse position  $y$  for different longitudinal positions  $x$  after Ref. 2. (d) NEGF-based calculated spin density in the diffusive regime as a function of transverse position  $y$  for different longitudinal positions  $x$  ( $L_S \approx 20 \text{ nm}$ ).

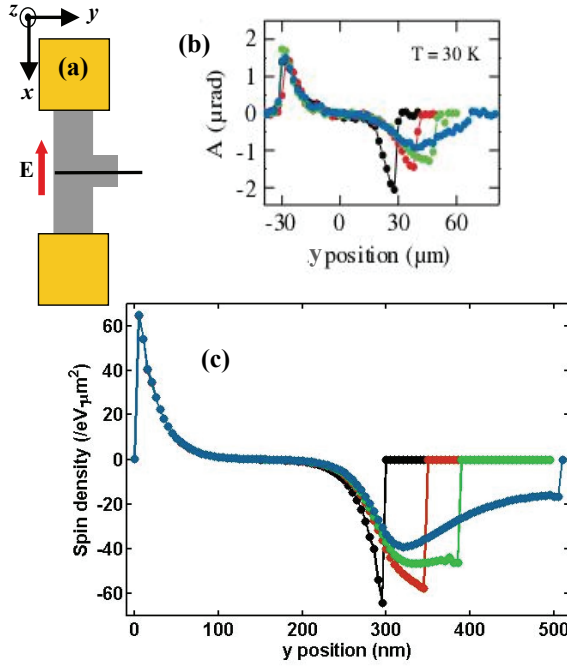


FIG. 3. (a) Schematic and experimental device geometry. (b) Kerr rotation as a function of position  $x$  for different side arm lengths after Ref. 2. (c) NEGF-based calculated spin density as a function of position  $x$  in diffusive regime for different side arm lengths ( $L_s=20\text{ nm}$ ).

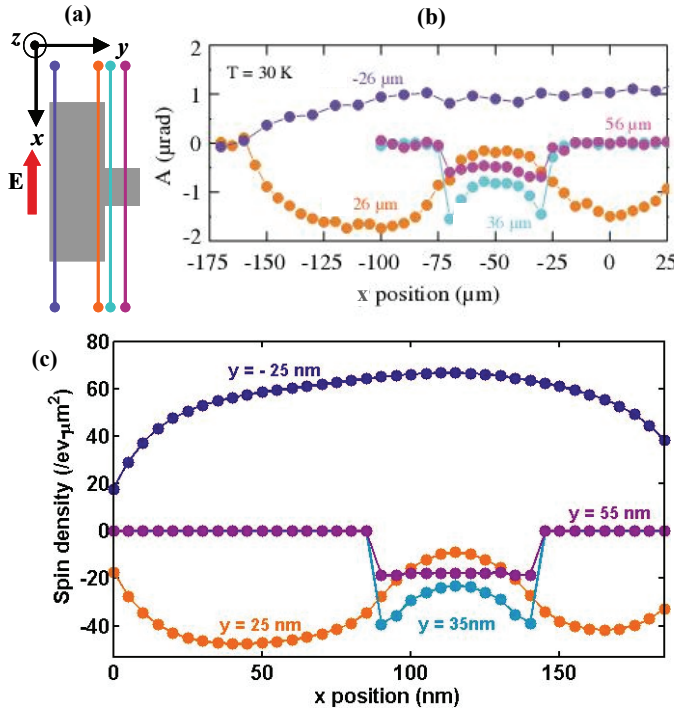


FIG. 4. (a) Schematic showing sample dimension. (b) Amplitude of Kerr rotation measured as a function of longitude position  $x$  for different transversal position  $y$  in the device after Ref. 2. (c) Calculated spin density in the diffusive regime as a function of longitude position  $x$  for different transversal position  $y$  ( $L_s=20\text{ nm}$ ).